Progress In Electromagnetics Research Letters, Vol. 107, 133–139, 2022

Design of a Plasmonic Metasurface for Refractive Index Sensing of Aqueous Glucose

Arslan Asim[1, *] and Michael Cada[1, 2]

Abstract—In this paper, a new plasmonic absorbing metasurface sensor has been proposed to determine glucose concentrations. Surface Plasmon Resonance (SPR) shift has been used as the indicator of glucose concentration. The sensor employs metal-dielectric-metal configuration along with metal nano-cylinders to provide near unity absorption in the near infrared wavelength range (1800–2200 nm). The absorption frequency shifts when the sensor is surrounded by materials of different refractive indices. The structure has been investigated through Finite Difference Time Domain (FDTD) simulations. The results show reflectance and absorbance peaks with different analyte concentrations. The sensor displays a linear response along with sensitivity and Figure of Merit (FOM) equal to almost 500 nm/RIU and 11.82 RIU^{-1}, respectively. The proposed sensor has potential applications in food and biomedical industries.

1. INTRODUCTION

Maxwell's equations provide a generalized framework for the propagation of electromagnetic waves. Maxwell's equations incorporate material properties of the medium. The key optical properties of a medium are permittivity (ε) and permeability (μ), which determine the refractive index (n). The refractive index, in turn, decides how the wave propagates through the medium. The dispersion equation given below summarizes this idea. It shows that the propagation constant (β) depends on the frequency (ω) and material properties [1].

$$\beta = \pm\omega\sqrt{\varepsilon\mu} \tag{1}$$

Conventionally, optical materials were considered to have positive ε and μ until Veselago described the electrodynamics of materials with simultaneous negative values of permittivity and permeability [2]. His work started to gain its real importance by the start of the twenty first century when a lot of exotic scientific phenomena were accomplished through the use of artificially engineered 'metamaterials' [3]. A groundbreaking achievement in this regard is the promising field of planar photonics [4]. Flat optics deals with ultrathin metamaterial surfaces containing a number of resonant nanostructures. These nanoresonators are smaller than the incident wavelengths of light. So, metasurfaces are basically 2 dimensional flat surfaces capable of manipulating light at sub-wavelength scale. Two classes of sub-wavelength nanostructures have been widely studied: plasmonic and dielectric structures. Theoretical and experimental works have proven their potential use in a huge variety of areas that include imaging, sensing, communications, healthcare, automotive, aerospace, and cloaking [5].

In the sensing domain, electromagnetic metasurfaces have shown tremendous prospects, especially with respect to the detection of minute biochemical molecules. Traditional sensing methods can be bulky, cumbersome, expensive, or time-consuming. Therefore, metasurfaces provide a suitable alternative platform for biosensing because of smaller footprint and rapid, label free detection [6, 7].

Received 4 September 2022, Accepted 2 November 2022, Scheduled 11 November 2022
* Corresponding author: Arslan Asim (arslanasim@dal.ca).
[1] Department of Electrical and Computer Engineering, Dalhousie University, Halifax, Canada. [2] IT4Innovations, VSB-Technical University of Ostrava, 17, Listopadu 15, 708 00, Ostrava-Poruba, Czech Republic.

Both plasmonic and dielectric surfaces have been used for a variety of sensing applications. However, a greater emphasis has been on the study of plasmonic biosensors. Plasmonic biosensors employ Surface Plasmon Resonance (SPR) at metal-dielectric interfaces. Free electrons present at the metal-dielectric interface experience coupling with the incident photons, giving rise to a Surface Plasmon Wave. The resonance conditions in plasmonic nanoantennas are affected by the refractive indices of surrounding materials. This results in frequency spectra shifts of plasmonic metasurfaces. Such shifts serve as sensing indicators. In the literature, this approach is termed as 'refractive index/refractometric sensing' [8].

Refractive index sensing has been applied to numerous problems. In [9], a highly sensitive plasmonic sensor has been proposed to identify blood groups. Different sensor designs have been used to study particular molecules like ethanol, hemoglobin, ether, ethylene glycol, quinolone, and chlorobenzene [10–13]. Cancer biomarkers have also been investigated using the refractometric technique [14]. A review paper presented by Patel et al. [15] has discussed the significance of metasurface biosensors for the detection of COVID 19 and other viruses. Graphene-based refractive index sensing has also shown promising results in latest works [16, 17]. An innovative design proposed by Hajshahvaladi et al. [18] has shown multi-wavelength tunability of a plasmonic refractive index sensor. Hybrid photonic crystal-plasmonic designs have also been proved worthwhile [19].

This paper focuses on the sensing of glucose in aqueous solution, through a metasurface made up of silver (Ag) and SiO_2. The refractive index of glucose changes with a change in concentration. Equation (2) describes the relationship between the concentration (C in g/100 mL) of glucose solution and the corresponding refractive index (n). The refractive index of water (n_w) equals 1.33 at room temperature [20].

$$n = n_w + 0.00143C \tag{2}$$

Ultrasensitive glucose sensing through nano-scale meta-optic sensors can have numerous applications in the food, biomedical and pharmaceutical industries. They can result in smaller device sizes, faster detection time, and simpler procedures. Therefore, this paper discusses the design of a glucose nano-sensor in detail by emphasizing its geometrical parameters and also reports the results when different glucose concentrations are placed above it. Based on the simulation results, the sensor response is found to be very sensitive and linear in the refractive index range (1.33–1.37).

2. MATERIALS AND METHODS

In this paper, a plasmonic metasurface biosensor has been designed and analyzed. The unit cell of the sensor is depicted by Figure 1. Four silver (Ag) nano-pillars stand on Ag layer. A layer of silicon dioxide is sandwiched between two Ag layers. The dimensions of the unit cell are as follows: $p_x = 420$ nm, $p_y = 420$ nm, $h = 300$ nm, $d = 120$ nm, $L_1 = 70$ nm, $L_2 = 40$ nm, and $L_3 = 90$ nm. Simulations have been carried out using Finite Difference Time Domain (FDTD) method to optimize the performance of the unit cell.

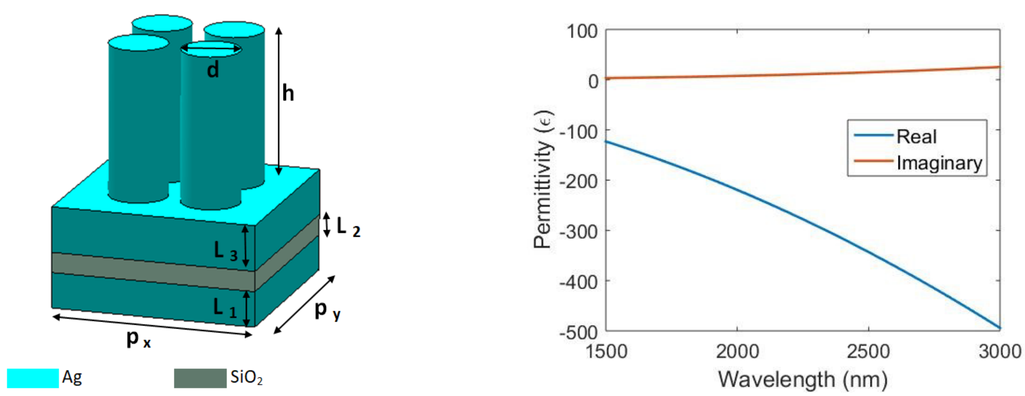

(a) (b)

Figure 1. (a) Sensor structure with dimension labels. (b) Ag permittivity (Drude model).

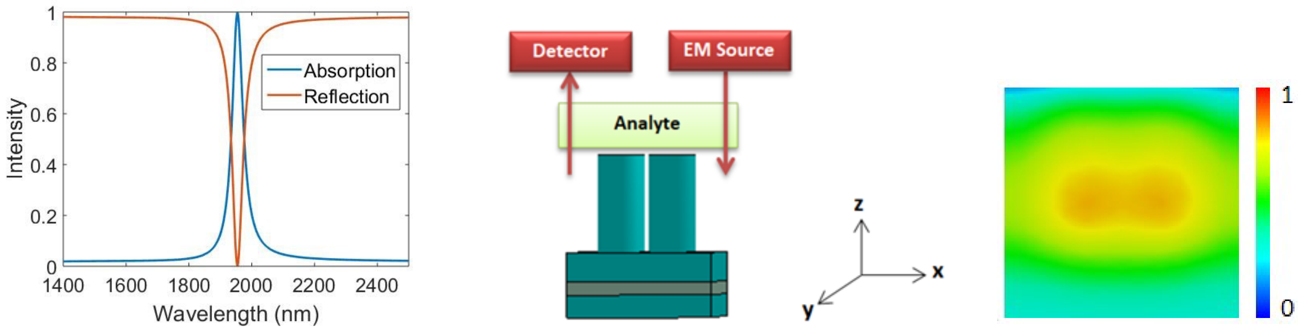

(a) (b) (c)

Figure 2. (a) Absorption and reflection spectra of the metasurface. (b) Schematic of sensing mechanism. (c) The electric field plot of the nano-cylinders at the absorption frequency (x-z cross-sectional view).

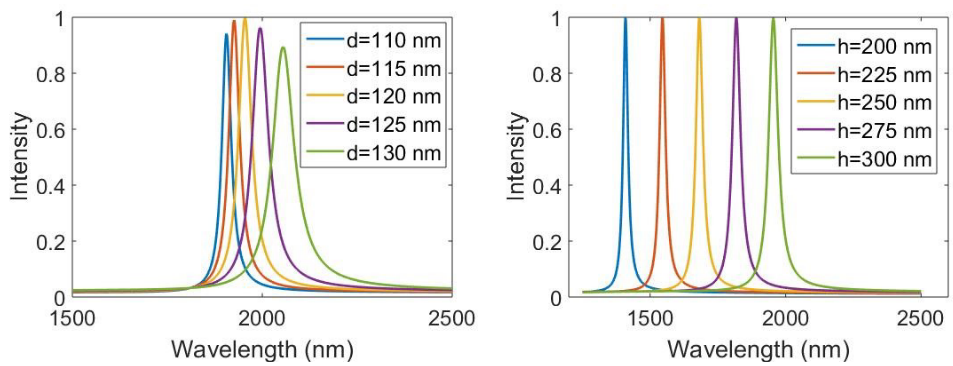

Figure 3. Effects of varying nano-cylinder parameters on the absorption peaks.

The metal-dielectric-metal configuration of the sensor allows increase in operating frequency, resulting in smaller device size. The use of plasmonic phenomenon achieves high sensitivity for a reflecting metasurface. To achieve the plasmonic effect, Ag has been used because it has smaller damping constant than other metals. A metasurface operating in the infrared regime can be designed at a smaller nanometer scale than terahertz (THz)/microwave metasurfaces.

The Drude model has been employed to implement dispersion properties of Ag [21]. The following values have been used for damping constant (γ) and plasma frequency (ω_p): $\gamma = 1.4(10^{16})\,\mathrm{s}^{-1}$, $\omega_p = 3.2(10^{13})\,\mathrm{s}^{-1}$. The electrical permittivity (ε) of Ag has also been plotted versus incident wavelength (λ). The permittivity of silicon dioxide is 3.75.

$$\varepsilon(\omega) = \left(1 - \frac{\omega_p^2}{\omega^2 + \gamma^2}\right) + j\left(\frac{\gamma\omega_p^2}{\omega(\omega^2 + \gamma^2)}\right) \tag{3}$$

Figure 2 presents the reflection and absorption spectra of the sensor in the near infrared region. The absorption ($A(\omega)$) and reflection ($R(\omega)$) coefficients can be derived from the S parameters of the unit cell [22]. The absorption coefficient of the metasurface goes to unity at one particular frequency in the infrared regime. The reflection and transmission coefficients approach zero where absorption becomes 1. The metasurface shows virtually no transmission on almost all frequencies.

$$A(\omega) = 1 - R(\omega) - T(\omega) \tag{4}$$

$$R(\omega) = |S_{11}|^2 \tag{5}$$

$$T(\omega) = |S_{21}|^2 \tag{6}$$

The geometrical parameters of the unit cell have been chosen to suit the particular requirements of the sensor. Figure 3 shows how the absorption peak shifts when the chosen parameters of the sensor design are changed. It can be seen that the diameter of the nano-cylinder is a critical parameter to be considered while fabricating the metasurface because the absorption level decreases as the diameter value is changed. On the other hand, the nanostructure height does not directly affect the absorption level. However, it changes the wavelength of peak absorbance. As a result, the height of the nano-resonators on the metasurface can be tuned between 200 nm and 300 nm to operate in different frequency sections within the infrared band.

3. RESULTS AND DISCUSSION

The sensor has been tested for different concentrations of glucose. The refractive indices of the glucose solutions have been derived from Equation (2). A layer of 150 nm over the sensor has been used to represent the aqueous solution. The shifts in the absorption peak have been observed and reported for different refractive indices of the glucose solution. The change in absorption peak wavelength ($\Delta\lambda$) with respect to the change in refractive index (Δn) and Full Width at Half Maximum (FWHM) of the sensor have been used to calculate the sensitivity (S), Figure of Merit (FOM), Quality factor (Q), Detection Limit (DL), and Detection Accuracy (DA). Table 1 shows the values of peak absorption for different refractive indices as well as the wavelengths at which those peaks occur. Figure 4 pictorially shows how the peaks shift when the glucose solution concentration changes.

Table 1. Summary of results for the sensor.

C (g/100 ml)	n	Absorption Peak Intensity	Absorption Peak Wavelength (nm)
0	1.33	0.9661	2104.4
5	1.33715	0.9637	2107.9
10	1.3443	0.9618	2111.5
15	1.35145	0.9597	2115.1
20	1.3586	0.9572	2118.6
25	1.36575	0.9547	2122.2

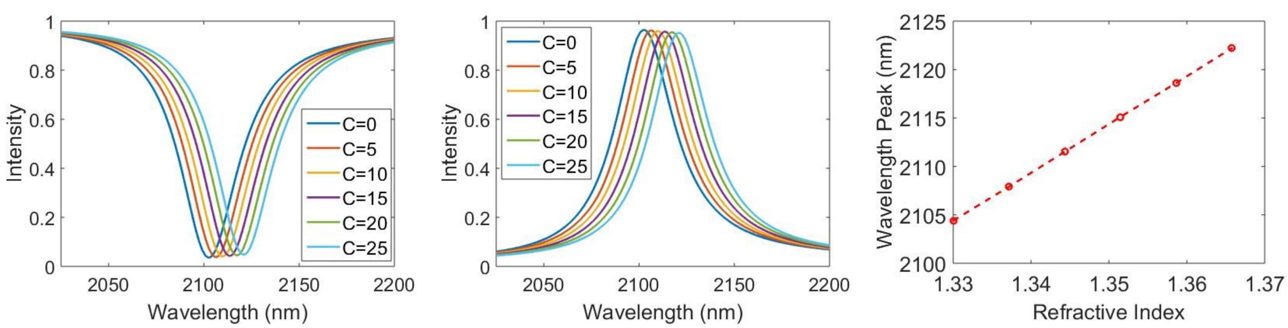

(a) (b) (c)

Figure 4. (a) Absorption and (b) reflection graphs for different concentrations of the glucose solution. (c) Absorption wavelength peak versus refractive index of the analyte.

The formulae for S, FOM, Q, DL, and DA are given below. Calculations have been performed using the data from Table 1 and the equations below. As a result, it is found that the proposed sensor has a sensitivity of around 500 nm/RIU (RIU stands for Refractive Index Unit). Using S, the FOM is found to be 11.82. The quality factor, detection limit, and detection accuracy are almost 50, 0.103 RIU, and $0.024\,\mathrm{nm}^{-1}$, respectively [23].

$$S = \frac{\Delta\lambda}{\Delta n} \tag{7}$$

$$\mathrm{FOM} = \frac{S}{\mathrm{FWHM}} \tag{8}$$

$$Q = \frac{\lambda_r}{\mathrm{FWHM}} \tag{9}$$

$$\mathrm{DL} = \left(\frac{\Delta n}{1.5}\right)\left(\frac{\mathrm{FWHM}}{\Delta\lambda}\right)^{1.25} \tag{10}$$

$$\mathrm{DA} = \frac{1}{\mathrm{FWHM}} \tag{11}$$

Table 2 provides a list of glucose metasurface sensors that have been proposed recently and compares them with the sensor proposed in this paper. The materials that have been used in the mentioned sensors include gold (Au), silver (Ag), copper (Cu), magnesium fluoride (MgF2), aluminum (Al), aluminum oxide (Al_2O_3), high density polyethylene (HDPE), polymethyl methacrylate(PMMA), silicon (Si), silicon dioxide (SiO_2), silicon nitride (Si_3N_4, SiN), and others as mentioned in the table. The structures mentioned in Table 2 have been investigated through numerical simulations. The experimental characterization can provide further insight into the sensor performance. Plasmonic nanostructures have been experimentally proven to be good candidates for biosensing applications [8].

Table 2. Research papers on glucose sensing.

REF.	**λ/f**	**MATERIALS**	**STRUCTURE**	**S**	**FOM**	**Q**
[24]	1400–2000 nm	Si, SiO_2	Nano-disk	230 nm/RIU	-	-
[25]	4–14 THz	Au, SiO_2, graphene	Cuboid	4.72 THz/RIU	14 RIU^{-1}	32.49
[26]	5–15 THz	Au, SiO_2, graphene	Cuboid	22.72 THz/RIU	34.96 RIU^{-1}	14.32
[27]	1300–1600 nm	Au, SiO_2, BK_7 glass	Nano-hole	1278 nm/RIU	168.1 RIU^{-1}	-
[28]	50–350 THz	Au	Split ring, nano-cylinders	4367 nm/RIU	-	-
[29]	50–300 THz	Au, Ag, Cu, Al, MgF_2, SiO_2, HPDE, Al_2O_3, PMMA	Nano-ring, nano-disk	225 nm/RIU	-	-
[30]	150–500 THz	Au, Ag, Cu, Al, MgF_2	Nanostructure with multiple layers and circular well for sensing material	300 nm/RIU	-	-
[31]	50–250 GHz	Al	S Shape	214 GHz/RIU	-	-
[32]	1200–1700 nm	Au, Si	Nano-bars	667 nm/RIU	38 RIU^{-1}	-
This letter	1800–2200 nm	Ag, SiO_2	Nano-cylinder	500 nm/RIU	11.82 RIU^{-1}	49.99

4. CONCLUSION

This paper discusses the role of metasurfaces as miniaturized, integrated optical sensing platforms. A metasurface has been designed with the aid of electromagnetic numerical simulations. The metasurface comprises silver and silica. The response of the sensor to different concentrations of glucose has been recorded. The sensor provides ultra-sensitive detection potential along with linear response. The sensor is polarization independent. This sensor can be an effective way to measure glucose concentration levels in the food industry. This work can be extended to carry out blood glucose level sensing, especially because blood serum is predominantly water. Future work on graphene-based glucose sensing can provide improved performance.

ACKNOWLEDGMENT

This work was supported by NSERC (Natural Sciences and Engineering Research Council) of Canada, and by the IT4Innovations National Supercomputing Center — Path to exascale project (EF16_013/0001791), of Czech Republic.

REFERENCES

1. Balanis, C. A., *Advanced Engineering Electromagnetics*, Wiley, New York, 1989.
2. Veselago, V. G., "The electrodynamics of substances with simultaneously negative values of ε and μ," *Sov. Phys. Uspekhi*, Vol. 10, No. 4, 509–514, 1968, doi: 10.1070/pu1968v010n04abeh003699.
3. Smith, D. R., J. B. Pendry, and M. C. K. Wiltshire, "Metamaterials and negative refractive index," *Science*, Vol. 305, 788–792, 2004.
4. Genevet, P., F. Capasso, F. Aieta, M. Khorasaninejad, and R. Devlin, "Recent advances in planar optics: From plasmonic to dielectric metasurfaces," *Optica*, Vol. 4, No. 1, 139, 2017, doi: 10.1364/optica.4.000139.
5. Li, A., S. Singh, and D. Sievenpiper, "Metasurfaces and their applications," *Nanophotonics*, Vol. 7, No. 6, 989–1011, 2018, doi: 10.1515/nanoph-2017-0120.
6. Chen, T., S. Li, and H. Sun, "Metamaterials application in sensing," *Sensors*, Vol. 12, No. 3, 2742–2765, 2012, doi: 10.3390/s120302742.
7. Zhang, S., et al., "Metasurfaces for biomedical applications: Imaging and sensing from a nanophotonics perspective," *Front. Opt. Photonics*, Vol. 10, No. 1, 265–299, 2021, doi: 10.1515/9783110710687-023.
8. Jin, C., Z. Wu, J. H. Molinski, J. Zhou, Y. Ren, and J. X. J. Zhang, "Plasmonic nanosensors for point-of-care biomarker detection," *Mater. Today Bio.*, Vol. 14, 100263, Jan. 2022, doi: 10.1016/j.mtbio.2022.100263.
9. Rakhshani, M. R. and M. A. Mansouri-Birjandi, "High sensitivity plasmonic refractive index sensing and its application for human blood group identification," *Sens. Actuators B, Chem.*, Vol. 249, 168–176, Oct. 2017.
10. Kabashin, A. V., et al., "Plasmonic nanorod metamaterials for biosensing," *Nat. Mater.*, Vol. 8, No. 11, 867–871, 2009, doi: 10.1038/nmat2546.
11. Alipour, A., A. Farmani, and A. Mir, "SiO_2-silver metasurface architectures for ultrasensitive and tunable plasmonic biosensing," *Plasmonics*, Vol. 15, No. 6, 1935–1942, Dec. 2020.
12. Vafapour, Z., A. Keshavarz, and H. Ghahraloud, "The potential of terahertz sensing for cancer diagnosis," *Heliyon*, Vol. 6, No. 12, Dec. 2020, Art. no. e05623.
13. Tavousi, A., M. R. Rakhshani, and M. A. Mansouri-Birjandi, "High sensitivity label-free refractometer based biosensor applicable to glycated hemoglobin detection in human blood using all-circular photonic crystal ring resonators," *Opt. Commun.*, Vol. 429, 166–174, Dec. 2018.
14. Son, H., S.-J. Kim, J. Hong, J. Sung, and B. Lee, "Design of highly perceptible dual-resonance all-dielectric metasurface colorimetric sensor via deep neural networks," *Scientific Reports*, Vol. 12, No. 1, Dec. 2022, doi: 10.1038/s41598-022-12592-9.
15. Patel, S. K., J. Surve, J. Parmar, K. Ahmed, F. M. Bui, and F. A. Al-Zahrani, "Recent advances in biosensors for detection of COVID-19 and other viruses," *IEEE Rev. Biomed. Eng.*, 1–16, 2022, doi: 10.1109/RBME.2022.3212038.
16. Patel, S. K., et al., "Encoding and tuning of THz metasurface-based refractive index sensor with behavior prediction using XGBoost regressor," *IEEE Access*, 2022, doi: 10.1109/ACCESS.2022.3154386.
17. Patel, S. K., J. Surve, J. Parmar, A. Natesan, and V. Katkar, "Graphene-based metasurface refractive index biosensor for hemoglobin detection: Machine learning assisted optimization," *IEEE Trans. Nanobioscience*, 1–8, 2022, doi: 10.1109/TNB.2022.3201237.

18. Hajshahvaladi, L., H. Kaatuzian, M. Danaie, and Y. Karimi, "Design of a highly sensitive tunable plasmonic refractive index sensor based on a ring-shaped nano-resonator," *Opt. Quantum Electron.*, Vol. 54, No. 1, 1–17, 2022, doi: 10.1007/s11082-021-03431-8.
19. Hajshahvaladi, L., H. Kaatuzian, and M. Danaie, "Design of a hybrid photonic-plasmonic crystal refractive index sensor for highly sensitive and high-resolution sensing applications," *Phys. Lett. Sect. A Gen. At. Solid State Phys.*, Vol. 420, 127754, 2021, doi: 10.1016/j.physleta.2021.127754.
20. Son, H., S.-J. Kim, J. Hong, J. Sung, and B. Lee, "Design of highly perceptible dual-resonance all-dielectric metasurface colorimetric sensor via deep neural networks," *Scientific Reports*, Vol. 12, No. 1, Dec. 2022, doi: 10.1038/s41598-022-12592-9.
21. Li, Y., "Plasmonic optics: Theory and applications," *Plasmonic Opt. Theory Appl.*, 2017, doi: 10.1117/3.2263757.
22. Abdulkarim, Y. I., et al., "A review on metamaterial absorbers: Microwave to optical," *Front. Phys.*, Vol. 10, 1–18, Apr. 2022, doi: 10.3389/fphy.2022.893791.
23. Patel, S. K., J. Surve, and J. Parmar, "Detection of cancer with graphene metasurface-based highly efficient sensors," *Diam. Relat. Mater.*, Vol. 129, 109367, Sep. 2022, doi: 10.1016/j.diamond.2022.109367.
24. Zhong, J., P. Ghosh, and Q. Li, "All-dielectric metasurface refractive index sensor with microfluidics," *Journal of Physics: Conference Series*, Vol. 1838, No. 1, Mar. 2021, doi: 10.1088/1742-6596/1838/1/012001.
25. Karthikeyan, M., P. Jayabala, S. Ramachandran, S. S. Dhanabalan, T. Sivanesan, and M. Ponnusamy, "Tunable optimal dual band metamaterial absorber for high sensitivity THz refractive index sensing," *Nanomaterials*, Vol. 12, No. 15, 2693, Aug. 2022, doi: 10.3390/nano12152693.
26. Nejat, M. and N. Nozhat, "Ultrasensitive THz refractive index sensor based on a controllable perfect MTM absorber," *IEEE Sensors Journal*, Vol. 19, No. 22, 10490–10497, Nov. 2019, doi: 10.1109/JSEN.2019.2931057.
27. Hajshahvaladi, L., H. Kaatuzian, and M. Danaie, "A high-sensitivity refractive index biosensor based on Si nanorings coupled to plasmonic nanohole arrays for glucose detection in water solution," *Opt. Commun.*, Vol. 502, Jan. 2022, doi: 10.1016/j.optcom.2021.127421.
28. Zhang, H., Y. Cheng, and F. Chen, "Quad-band plasmonic perfect absorber using all-metal nanostructure metasurface for refractive index sensing," *Optik (Stuttg.)*, Vol. 229, Mar. 2021, doi: 10.1016/j.ijleo.2021.166300.
29. Vafapour, Z., "Polarization-independent perfect optical metamaterial absorber as a glucose sensor in food industry applications," *IEEE Trans. Nanobiosci.*, Vol. 18, No. 4, 622–627, Oct. 2019.
30. Vafapour, Z., et al., "The potential of refractive index nanobiosensing using a multi-band optically tuned perfect light metamaterial absorber," *IEEE Sensors J.*, early access, Apr. 2, 2021, doi: 10.1109/JSEN.2021.3070731.
31. Al-Naib, I., "Terahertz asymmetric S-shaped complementary metasurface biosensor for glucose concentration," *Biosensors (Basel)*, Vol. 12, No. 8, Aug. 2022, doi: 10.3390/bios12080609.
32. Sun, Y., L. Zhang, H. Shi, S. Cao, S. Yang, and Y. Wu, "Near-infrared plasma cavity metasurface with independently tunable double Fano resonances," *Results Phys.*, Vol. 25, 104204, Jun. 2021, doi: 10.1016/j.rinp.2021.104204.